

This copy is for your personal, non-commercial use only.

If you wish to distribute this article to others, you can order high-quality copies for your colleagues, clients, or customers by [clicking here](#).

Permission to republish or repurpose articles or portions of articles can be obtained by following the guidelines [here](#).

The following resources related to this article are available online at www.sciencemag.org (this information is current as of June 17, 2010):

Updated information and services, including high-resolution figures, can be found in the online version of this article at:

<http://www.sciencemag.org/cgi/content/full/328/5985/1554>

Supporting Online Material can be found at:

<http://www.sciencemag.org/cgi/content/full/328/5985/1554/DC1>

This article **cites 20 articles**, 3 of which can be accessed for free:

<http://www.sciencemag.org/cgi/content/full/328/5985/1554#otherarticles>

This article has been **cited by** 1 articles hosted by HighWire Press; see:

<http://www.sciencemag.org/cgi/content/full/328/5985/1554#otherarticles>

This article appears in the following **subject collections**:

Anthropology

<http://www.sciencemag.org/cgi/collection/anthro>

Radiocarbon-Based Chronology for Dynastic Egypt

Christopher Bronk Ramsey,^{1*} Michael W. Dee,¹ Joanne M. Rowland,¹ Thomas F. G. Higham,¹ Stephen A. Harris,² Fiona Brock,¹ Anita Quiles,³ Eva M. Wild,⁴ Ezra S. Marcus,⁵ Andrew J. Shortland⁶

The historical chronologies for dynastic Egypt are based on reign lengths inferred from written and archaeological evidence. These floating chronologies are linked to the absolute calendar by a few ancient astronomical observations, which remain a source of debate. We used 211 radiocarbon measurements made on samples from short-lived plants, together with a Bayesian model incorporating historical information on reign lengths, to produce a chronology for dynastic Egypt. A small offset (19 radiocarbon years older) in radiocarbon levels in the Nile Valley is probably a growing-season effect. Our radiocarbon data indicate that the New Kingdom started between 1570 and 1544 B.C.E., and the reign of Djoser in the Old Kingdom started between 2691 and 2625 B.C.E.; both cases are earlier than some previous historical estimates.

Egyptian historical chronologies have been underpinned by relative dating derived from a variety of sources. Building on the surviving evidence from Manetho's *Aegyptiaca* (written in the third century B.C.E.) and the king lists dating from the pharaonic era, generations of scholars have used written and archaeological information to check, and in some instances revise, the sequence of kings and the lengths of their reigns. Undocumented years at the ends of some reigns and overlap between successive monarchs create uncertainties of the order of a few years (1).

The placement of this relative chronology on the absolute-calendar time scale, however, has been principally based on the interpretation of a small number of ancient astronomical observations in the Middle and New King-

doms (MK and NK, respectively) and is therefore considerably less certain. Many of the relevant celestial and lunar phenomena repeat at regular intervals, giving different possible chronologies, and their timing is dependent on the location of the observer, which may also add to the uncertainty (2). In addition, much work has been done to synchronize the chronology of Egypt to that of neighboring civilizations (3–5), particularly with Mesopotamia, which also has a rich and detailed historical record and astronomically based datums; however, precise absolute-age synchronisms between them are only possible in the late NK (6). Radiocarbon dating, which is a two-stage process involving isotope measurements and then calibration against similar measurements made on dendrochronologically dated wood,

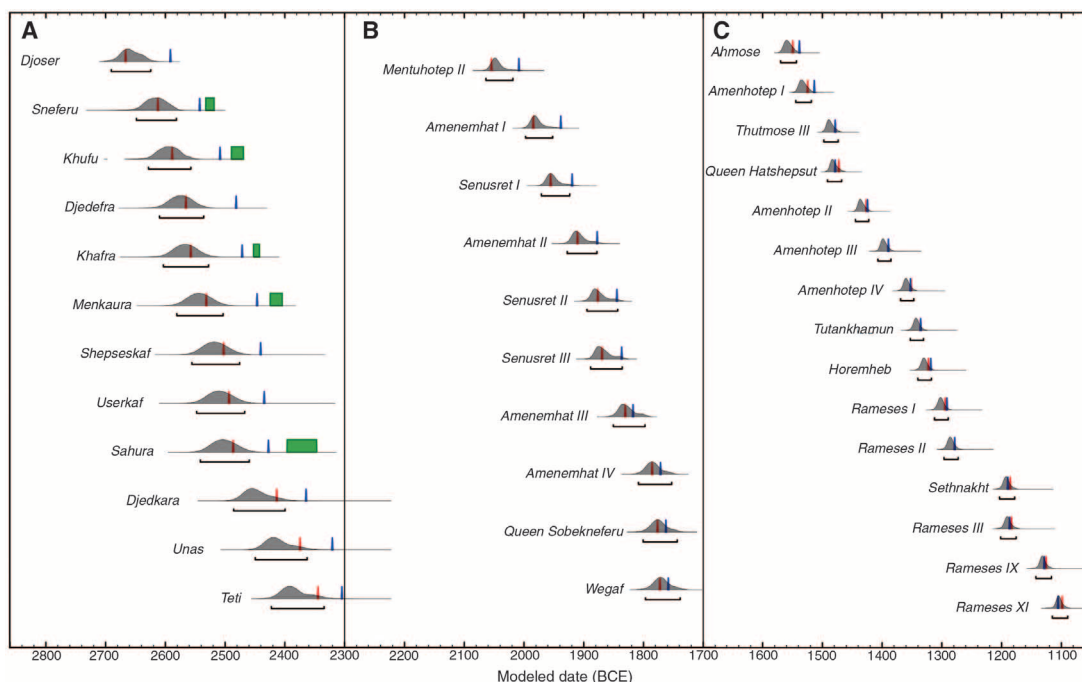
usually gives age ranges of 100 to 200 years for this period (95% probability range) and has previously been too imprecise to resolve these questions.

Here, we combine several classes of data to overcome these limitations in precision: measurements on archaeological samples that accurately reflect past fluctuations in radiocarbon activity, specific information on radiocarbon activity in the region of the Nile Valley, direct linkages between the dated samples and the historical chronology, and relative dating information from the historical chronology. Together, these enable us to match the patterns present in the radiocarbon dates with the details of the radiocarbon calibration record and, thus, to synchronize the scientific and historical dating methods. We obtained short-lived plant remains from museum collections (e.g., seeds, basketry, plant-based textiles, plant stems, fruits) that were directly associated with particular reigns or short sections of the historical chronology. We avoided charcoal and wood samples because of the possibility of inbuilt

¹Research Laboratory for Archaeology and the History of Art, University of Oxford, Dyson Perrins Building, South Parks Road, Oxford OX1 3QY, UK. ²Department of Plant Sciences, University of Oxford, South Parks Road, Oxford OX1 3RB, UK. ³Laboratoire de Mesure du Carbone 14, bat 450 Porte 4E, Commissariat à l'Énergie Atomique (CEA)–Saclay, France–Université Paris VII–Diderot, 91191 Gif-Sur-Yvette, France. ⁴Vienna Environmental Research Accelerator Laboratory, Fakultät für Physik, Isotopenforschung, Universität Wien, Währingerstrasse 17, A-1090 Wien, Austria. ⁵The Recanati Institute for Maritime Studies, University of Haifa, Haifa 31905, Israel. ⁶Centre for Archaeological and Forensic Analysis, Department of Applied Science, Security and Resilience, Cranfield University, Shrivvenham, Swindon SN6 8LA, UK.

*To whom correspondence should be addressed. E-mail: christopher.ramsey@rlaha.ox.ac.uk

Fig. 1. A selection of the accession dates (first regnal year) for the (A) OK, (B) MK, and (C) NK derived from this research. The marginal posterior probability distributions are shown in gray, with their corresponding 95% probability ranges indicated below. Red, historical dates from Shaw (18); blue, from Hornung *et al.* (21); and green, from Spence (24). The accession intervals used for the model are from Shaw (18), and corresponding distributions using the intervals from Hornung *et al.* (21) are shown in fig. S4.



age. We also avoided mummified material because of concerns about contamination from bitumen or other substances used in the mummification process and human material because of the possibility of riverine or marine components in the diet (which might contain older carbon). We selected samples according to the security of their archaeological context and relation to a given king's reign, but in making the chronological associations, we were reliant on the judgement of excavators and curators and on the integrity of the collections themselves, because many of the excavations took place in the 19th or early 20th century. Most of the samples were taken from individual funerary contexts. In a few cases, we sampled different short-lived plant remains from a single context, allowing us to check the internal consistency of the measurements.

We prepared samples for radiocarbon analysis using standard acid-base-acid methods, in some cases preceded by solvent extraction of possible museum-based contaminants (7–10). Next, we converted treated samples to graphite (11) before radiocarbon measurement by accelerator mass spectrometry (AMS) (12–14). Calibration of the radiocarbon dates was against the InCal04 calibration curve (15) using OxCal v4.1.3 (16, 17). In all, we obtained 211 AMS radiocarbon determinations (table S1). Where there were indications of conservation work, we attempted to avoid sampling the affected areas and used solvent pretreatment methods to remove potential contaminants, but the pos-

sibility remains that some cases of contamination may have escaped detection.

Fourteen of the ancient samples were actually from the first or second millennium C.E. and were thus clearly intrusive; we do not consider these further. Another small set of radiocarbon dates show offsets of a few hundred years (typically younger than expected). This is not surprising, as tomb contexts are often disturbed after being sealed, and some intrusion of younger material is always a possibility. Where we have multiple samples from single contexts, the internal agreement between the dates is usually good, except for two measurements on the same sample, where we suspect contamination, that are not included in the analysis (see table S1 for details).

In one case, although the internal consistency is satisfactory, seven dates from one single 19th Dynasty tomb are ~200 years older than the historical age ascribed to them (see dates ascribed to Ramses I/Seti I in table S1). In this instance, we have concluded that there must be an archaeological problem and have excluded the dates from the model. We included all other dates (188 in total), whether or not they appear to be outliers in our analysis. We have 128 dates from the NK, 43 from the MK, and 17 from the Old Kingdom (OK). The majority (~75%) of the measurements have calibrated age ranges that overlap with the conventional historical chronology, within the wide error limits that result from the calibration of individual dates.

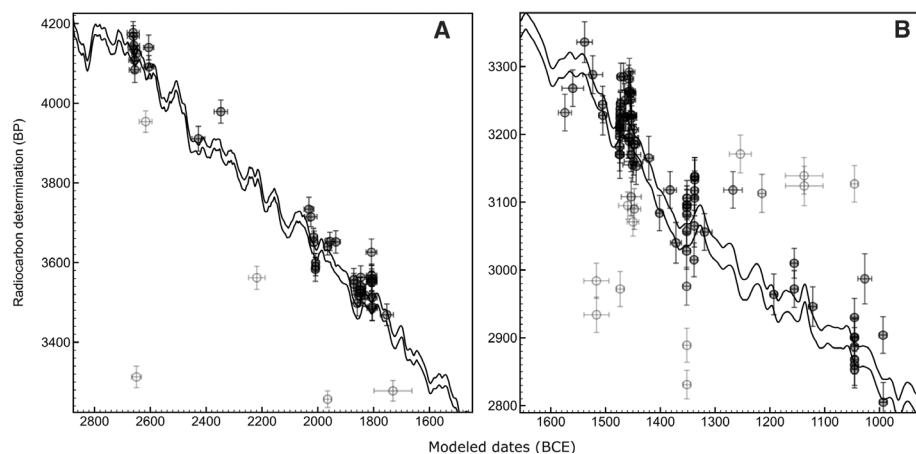


Fig. 2. This figure shows the distribution of uncalibrated radiocarbon dates against the modeled age. For each measurement, we show the mean and $\pm 1\sigma$ of the radiocarbon and modeled calendar dates: Points that have a low likelihood of being an outlier are shown with gray points and black error bars; those that are certain to be outliers are shown with gray error bars and white points (see table S1 for outlier probabilities). The calibration curve is shown as two black lines ($\pm 1\sigma$). The dates from the OK [(A) up to ~2300 B.C.E.] are concentrated in particular parts of the chronology; most of the information comes from the start of the OK. For the MK [(A) from ~2100 B.C.E.], the pattern of radiocarbon dates clearly reflects the distribution in the calibration curve, picking up distinctive features present 1800 to 1900 B.C.E. and ~2000 B.C.E. (B) There are many more dates shown in the NK, most of which are superimposed on each other and overlie the calibration curve, picking up clear distinctive features of the curve, for example, around 1450 B.C.E. There is also a scatter of outliers (shown in gray), but these show no systematic pattern and have no single explanation.

To build a high-precision chronological sequence, we combined our radiocarbon measurements with the historical information relating to reign order and length. To do this, we adopted a Bayesian modeling approach using the program OxCal (16, 17). For each major period (OK, MK, and NK), we constructed a separate multiphase model (16) with phase boundaries set at the accession dates for the individual rulers (or, in some cases, series of rulers). The order of the reigns was defined but no prior information was included on the absolute dating of the chronology. The dates for the samples were constrained to lie in particular reigns (or, in some instances, within several adjacent reigns), and their associated calibrated radiocarbon measurements were included as likelihoods in the Bayesian model. The radiocarbon dates thus provide the only linkage in the model to the calendar time scale.

We also included reign lengths as prior information relating to the intervals between the successive accession dates, using the consensus values from Shaw (18) as our estimates. Uncertainties in reign lengths are small, especially for the NK where they are typically 1 or 2 years, though larger in a few specific cases such as for Thutmose II and Horemheb. We quantify this uncertainty in our model, but rather than using the distribution $N(0,1^2)$, we use the Student's t distribution ($\nu = 5$), which has longer tails to provide a more robust result. For the MK, we use an uncertainty that is three times that of the NK [i.e., similar to a longer-tailed $N(0,3^2)$]; for the OK, the uncertainty is five times that of the NK. These uncertainties are somewhat subjective, so we tested the models for robustness under different choices of the scaling of these uncertainties (fig. S2).

We also used environmental information from a series of 66 AMS measurements on botanical specimens, with documented dates of collection from Egypt in the period 1700 to 1900 C.E. These show a small but significant depletion in radiocarbon levels relative to the calibration curve (15), equivalent to a shift to older radiocarbon dates of 19 ± 5 radiocarbon years ($^{14}\text{C yr}$) (19). This offset most likely reflects the unusual growing season in pre-modern Egypt, which was concentrated during the winter months after the annual inundation. Plants in Egypt sampled the atmosphere at a different time of the year than the trees measured for the calibration curve, and we might expect a slight depletion because of the annual fluctuation in the atmospheric radiocarbon activity. The size of the effect agrees well with the estimated peak-to-peak amplitude of the seasonal fluctuations in radiocarbon activity in the atmosphere of up to 4 per mil ($<32 \text{ }^{14}\text{C yr}$) for the pre-industrial era, produced by variations in the rate of transport of ^{14}C from the stratosphere to the troposphere (20). We used a single model parameter (ΔR) to model the environmental offset, with a prior of $N(19,5^2)$.

Because a proportion of the samples were expected to be out of context, we used *t*-type outlier-modeling (17) with a prior outlier probability of 5%; we also tested the outcomes of the model for robustness with a higher value of this prior probability (see supporting online material).

The modeling of the data provides a chronology that extends from ~2650 to ~1100 B.C.E. (Figs. 1 and 2 and Table 1). The benefits of using the reign order and length information together with the radiocarbon dates are greatest where density of dates is highest. In the NK (128 dates), the average calendrical precision is 24 years [95% highest posterior density (hpd) range] for accession dates (or 11 years for the 68% hpd range). In the MK, where dates are sparser and the uncertainty in the reign lengths is greater, the average calendrical precision is 53 years (95%); in the OK, where the number of dates is even lower, the precision is 76 years (95%) but is still markedly better than that possible with individual measurements. Because reign length has been included in our models, it is important to stress that the outputs of the models cannot be used to provide reign-length information.

The radiocarbon-based chronology for the NK resolves different possible historical chronologies (Fig. 1C). The radiocarbon dates chosen for the NK are on samples from the 17th to the 21st Dynasties, which provide brackets beyond the beginning and end of the NK. However, there are no dates for specific reigns before that of Thutmose III, and so dates earlier than this are based primarily on the reign-length information included in the model. The agreement is closest to the consensus chronology compiled by Shaw (18), in which the NK starts in 1550 B.C.E. and from which we take our reign lengths. It rules out some of the other interpretations proposed (21–23) that are somewhat later, even if different reign lengths and overlaps are considered (fig. S3A). The radiocarbon dates imply that the NK might have begun earlier by about a decade than the consensus date of Shaw, which would imply either shorter overlaps or a slight extension to some reigns in the sequence.

In the MK, the conventional (and earlier) historical chronology (1) is largely based on a single observation of the heliacal rising of the star Sothis (Sirius). Different interpretations of this and other astronomical observations are possible, depending on the supposed point of observation, and a chronology that is about 40 years younger has also been put forward, based more on lunar observations (21–23). The radiocarbon chronology favors the earlier interpretation, but it cannot be used to decide conclusively between these interpretations (Fig. 1B).

The results for the OK, although lower in resolution, also agree with the consensus chronology of Shaw (18) but have the resolution to contradict some suggested interpretations of the

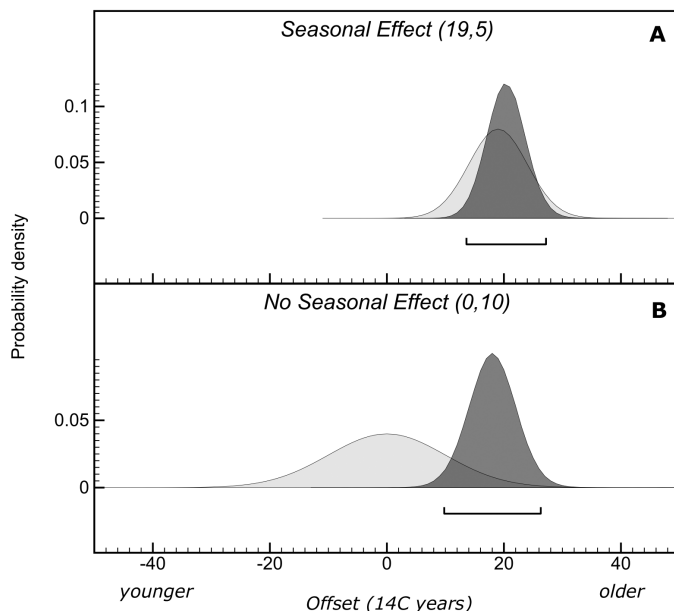
Table 1. Modeled accession dates (first regnal year) for selected kings and queens in the Egyptian historical chronology based on the new radiocarbon data (this paper) and reign accession intervals from Shaw (18) (see tables S7 and S8 for full lists) compared with other estimates (18, 21). The number of radiocarbon dates for individual reigns included in the models is shown (full details are in table S1). 0, reigns for which we have no dates; ND, not determined.

King/queen	No. ¹⁴ C dates in models	Accession dates (B.C.E.)					
		Shaw (18)	Hornung et al. (21)	Modeled hpd ranges			
				68%		95%	
				from	to	from	to
<i>Old Kingdom</i>							
Djoser	7	2667	2592	2676	2643	2691	2625
Sneferu	2	2613	2543	2634	2599	2649	2582
Khufu	0	2589	2509	2613	2577	2629	2558
Djedefra	0	2566	2482	2593	2556	2610	2536
Khafra	0	2558	2472	2586	2548	2604	2528
Menkaura	0	2532	2447	2564	2524	2581	2504
Shepseskaf	0	2503	2441	2538	2498	2556	2476
Userkaf	0	2494	2435	2530	2489	2548	2468
Sahura	0	2487	2428	2524	2482	2542	2460
Djedkara	1	2414	2365	2473	2432	2486	2400
Unas	0	2375	2321	2438	2397	2450	2363
Teti	0	2345	2305	2412	2370	2423	2335
	7			Further dates from the Second to Eighth Dynasties			
<i>Middle Kingdom</i>							
Mentuhotep II	9	2055	2009	2057	2040	2064	2019
Amenemhat I	4	1985	1939	1991	1973	1998	1952
Senusret I	1	1956	1920	1965	1945	1971	1924
Amenemhat II	0	1911	1878	1922	1901	1928	1878
Senusret II	2	1877	1845	1890	1868	1895	1844
Senusret III	10	1870	1837	1884	1860	1889	1836
Amenemhat III	10	1831	1818	1844	1820	1851	1798
Amenemhat IV	0	1786	1772	1799	1773	1809	1753
Sobekneferu	0	1777	1763	1790	1764	1801	1744
Wegaf	0	1773	1759	1785	1758	1797	1739
	7			Further dates from the 11th to 13th Dynasties			
<i>New Kingdom</i>							
Ahmosé	0	1550	1539	1566	1552	1570	1544
Amenhotep I	0	1525	1514	1541	1527	1545	1519
Thutmose III	24	1479	1479	1494	1483	1498	1474
Hatshepsut	25	1473	1479	1488	1477	1492	1468
Amenhotep II	1	1427	1425	1441	1431	1445	1423
Amenhotep III	2	1390	1390	1404	1393	1408	1386
Amenhotep IV	17	1352	1353	1365	1355	1370	1348
Tutankhamun	7	1336	ND	1349	1338	1353	1331
Horemheb	0	1323	1319	1336	1325	1341	1318
Rameses I	0	1295	1292	1308	1297	1313	1290
Rameses II	2	1279	1279	1292	1281	1297	1273
Sethnakht	0	1186	1190	1198	1187	1204	1179
Rameses III	0	1184	1187	1196	1185	1202	1176
Rameses IX	2	1126	1129	1137	1127	1143	1117
Rameses XI	0	1099	1106	1110	1100	1116	1090
	48			Further dates from the 17th to 21st Dynasties			

evidence, such as the astronomical hypothesis of Spence (24), which is substantially later, or the reevaluation of this hypothesis (25), which leads to a date that is earlier. The absence of astronomical observations in the papyrological record for the OK means that this data set provides one of the few absolute references for the positioning of this important period of Egyptian history (Fig. 1A).

Thus, the radiocarbon measurements provide a coherent chronology for ancient Egypt, which is in good agreement with some earlier attempts to tie down the floating chronology. In contrast, a previous large-scale radiocarbon study gave dates that were substantially earlier than the expected ages for the OK (26) and dates that are earlier than expected at Tell el-Dab^ca (27). These discrepancies probably reflect the choice

Fig. 3. Systematic regional offset in radiocarbon dates from the calibration curve. **(A)** In our model, we have used a prior for the regional offset of 19 ± 5 ^{14}C yr, as shown by the light gray region; the posterior density for the NK (dark gray region) confirms the assumed value for this period. **(B)** If we use a much more neutral prior for this offset of 0 ± 10 , the posterior for this parameter is almost unchanged, showing that the ancient data support such an offset independently.



of samples for dating. Many of the sites in ancient Egypt were densely populated over long periods (a notable exception being Amarna). In addition, some resources, such as wood, were in short supply. Reuse of scarce resources can result in the incorporation of older organic material, particularly wood and charcoal, into younger deposits. The long use, revisiting, and robbing of some monuments also provide opportunities for later organic material to be discovered in earlier contexts. We were able to reduce, but not eliminate, such outliers by selecting only short-lived plants from secure contexts. Despite these precautions, we still found a significant number of young outliers among the dates measured, which we accounted for by using Bayesian outlier analysis.

To test the sensitivity of our analysis to the parameters of the model, we looked at the effect of altering the uncertainty in the reign lengths, alternative reign-length estimates (21), and the prior outlier probability (figs. S2 to S4). We also evaluated the effect of applying a different prior for ΔR . The main model uses a prior of $N(19, 5^2)$, based on the environmental information (19). If we use a more neutral prior of $N(0, 10^2)$ for the NK where we have most dates, the chronology is virtually unaltered (fig. S5), and the posterior for ΔR is also similar (Fig. 3). This shows that the ancient samples independently confirm a local offset in radiocarbon of 20 ± 5 years, because the pattern of radiocarbon dates found through the NK fits better with the calibration curve when such an offset is applied.

The confirmation of a small regional offset will need to be considered in the calibration of all radiocarbon dates from the Nile region. The small size of this offset implies that previous studies that have seen much larger offsets (26, 27) are probably due to sample selection or context.

This radiocarbon-based chronology for the dynastic period allows direct comparison to the radiocarbon records of predynastic sites in Egypt, and those from the neighboring regions of Libya and Sudan, which is a prerequisite for understanding the speed and mechanisms of Egyptian state formation. This chronology also has implications for the wider Mediterranean and surrounding regions that rely on linkages to Egypt to anchor their own chronologies (3–5). For the second millennium B.C., for example, it will contribute to our understanding of the differences between the historical Aegean chronology, derived from linkages with Egypt (27), and the radiocarbon record for that region, and specifically, for the Minoan eruption of Santorini (28, 29). More widely, Egypt and Mesopotamia are the only parts of the western Old World that have written records spanning the Bronze and Iron ages, and they are linked by trade with regions that stretch from Central Asia to the western Mediterranean and down into Nubia. Chronology is key to understanding the nature of these linkages, and the harmonization of the historical chronologies of Egypt with the calibrated radiocarbon time scale removes a fault line between regions dated scientifically and those tied into historical sequences.

References and Notes

1. W. A. Ward, *Bull. Am. Schools Orient. Res.* **288**, 53 (1992).
2. K. A. Kitchen, *World Archaeol.* **23**, 201 (1991).
3. M. Bietak, Ed., *The Synchronisation of Civilizations in the Eastern Mediterranean in the Second Millennium BC* (Verlag der Österreichischen Akademie der Wissenschaften, Vienna, 2001).
4. M. Bietak, Ed., *The Synchronisation of Civilizations in the Eastern Mediterranean in the Second Millennium BC II* (Verlag der Österreichischen Akademie der Wissenschaften, Vienna, 2003).
5. M. Bietak, E. Czerny, Eds., *The Synchronisation of Civilisations in the Eastern Mediterranean in the Second Millennium BC III* (Verlag der Österreichischen Akademie der Wissenschaften, Vienna, 2007).

6. K. A. Kitchen, in (5), pp. 163–171.
7. F. Brock, T. F. G. Higham, P. Ditchfield, C. Bronk Ramsey, *Radiocarbon* **52**, 103 (2010).
8. E. M. Wild et al., *Radiocarbon* **50**, 1 (2008).
9. Q. Hua et al., *Nucl. Instrum. Methods Phys. Res. B* **223–224**, 489 (2004).
10. F. Bruhn, A. Duhr, *Radiocarbon* **43**, 229 (2001).
11. M. Dee, C. Bronk Ramsey, *Nucl. Instr. Methods Phys. Res. B* **172**, 449 (2000).
12. C. Bronk Ramsey, T. Higham, P. Leach, *Radiocarbon* **46**, 17 (2004).
13. E. Cottreau et al., *Radiocarbon* **49**, 291 (2007).
14. P. Steier, F. Dellinger, W. Kutschera, W. Rom, E. M. Wild, *Radiocarbon* **46**, 5 (2004).
15. P. J. Reimer et al., *Radiocarbon* **46**, 1029 (2004).
16. C. Bronk Ramsey, *Radiocarbon* **51**, 337 (2009).
17. C. Bronk Ramsey, *Radiocarbon* **51**, 1023 (2009).
18. I. Shaw, Ed., *The Oxford History of Ancient Egypt* (Oxford Univ. Press, Oxford, 2000).
19. M. W. Dee et al., *J. Archaeol. Sci.* **37**, 687 (2009).
20. B. Kromer et al., *Science* **294**, 2529 (2001).
21. E. Hornung, R. Krauss, D. A. Warburton, Eds., *Ancient Egyptian Chronology* (Brill, Leiden, Netherlands, 2006).
22. D. Franke, *Orientalia* **57**, 113 (1988).
23. R. Krauss, *Sothis- und Monddaten: Studien zur astronomischen und technischen Chronologie altägyptens* (Gerstenberg, Hildesheim, Germany, 1985).
24. K. Spence, *Nature* **408**, 320 (2000).
25. D. Rawlins, K. Pickering, *Nature* **412**, 699 (2001).
26. G. Bonani et al., *Radiocarbon* **43**, 1297 (2001).
27. M. Bietak, F. Höflmayer, in *The Synchronisation of Civilisations in the Eastern Mediterranean in the Second Millennium BC III*, M. Bietak, E. Czerny, Eds. (Verlag der Österreichischen Akademie der Wissenschaften, Vienna, 2007), pp. 13–23.
28. S. W. Manning et al., *Science* **312**, 565 (2006).
29. W. L. Friedrich et al., *Science* **312**, 548 (2006).
30. This project was funded by the Leverhulme Trust (grant no. F/08 622/A). The botanical specimens were from the Oxford University Herbaria and the Natural History Museum, London. Archaeological samples were from Ägyptisches Museum und Papyrussammlung, Berlin; Ashmolean Museum, Oxford; Bolton Museum and Art Gallery; British Museum, London; City Museum and Art Gallery, Bristol, UK; Cornell University, New York; Desert Research Institute, Las Vegas, Nevada; Kunsthistorisches Museum, Vienna; The Manchester Museum; Medelhavsmuseet, Stockholm; Metropolitan Museum of Art, New York; Musée du Louvre, Paris; Musées royaux d'art et d'histoire, Brussels; National Museums, Liverpool, UK; The Petrie Museum of Egyptian Archaeology, London; The Pitt Rivers Museum, Oxford; Royal Botanic Gardens, Kew, UK; Staatliches Museum Ägyptischer Kunst, Munich; and the Victoria Museum of Egyptian Antiquities, Uppsala University, Sweden. The Oxford laboratory infrastructure was funded by the Natural Environment Research Council and software development by English Heritage. The Illahun, Heqanakht, and Hatshepsut measurements and research were funded by the German-Israeli Foundation for Scientific Research and Development (grant no. I-2069-1230.4/2004); preliminary background research was aided by the SCIEM2000 project. The dating at Saclay was performed at the LMC14 (funded by CNRS, CEA, Institut de Radioprotection et de Sécurité Nucléaire, Institut de Recherche pour le Développement, and Ministère de La Culture).

Supporting Online Material

www.sciencemag.org/cgi/content/full/328/5985/1554/DC1
 Materials and Methods
 SOM Text
 Figs. S1 to S5
 Tables S1 to S7
 References

10 March 2010; accepted 3 May 2010
 10.1126/science.1189395

Downloaded from www.sciencemag.org on June 17, 2010